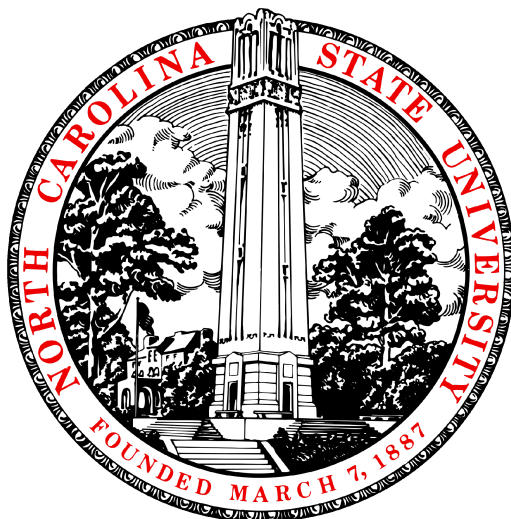


NE533 Fuel Performance MOOSE Project Writeup Part 1 + Part 2

TSU-CHUN TENG 200543795

Professor: Dr. Benjamin Beeler



DEPARTMENT OF NUCLEAR ENGINEERING
NORTH CAROLINA STATE UNIVERSITY

March 29, 2024

Table of contents

1	Introduction	1
2	Methods	2
2.1	Part 1	2
2.1.1	The parameters, meshing methods, and other details	2
2.2	Part 2	4
2.2.1	The parameters, meshing methods, and other details	5
3	Results	6
3.1	Part 1	6
3.1.1	Analytical solution of steady state with constant k	6
3.1.2	MOOSE Results	7
3.1.3	Discussion	10
3.2	Part 2	11
3.2.1	MOOSE Results	11
3.2.2	Discussion	13
4	Conclusion	14

Chapter 1

Introduction

In the NE533 Nuclear Fuel Performance course, we learned about numerous properties and calculations relevant to nuclear fuels, particularly for Light Water Reactors (LWRs). However, simply acquiring knowledge in class is insufficient; understanding its practical applications and utilizing simulation tools to solve real-world problems are crucial aspects. Therefore, the motivation behind this project is to deepen our comprehension of the key concepts covered in this course.

In Part 1, I developed the initial MOOSE input file and attempted to address the problem of monitoring the impact of fuel center-line temperature under both Steady and Transient States, considering constant thermal conductivity and temperature-dependent conductivity.

In Part 2, our focus shifts to examining the impact of introducing coolant into the system. Additionally, we utilized the "GapHeatTransfer" feature within the ThermalContact block (which can be seen as a type of boundary condition) to simulate the heat transferred across unmeshed gaps between two different blocks, rather than directly calculating it from our mesh.

Chapter 2

Methods

In this section, I will outline the important methods, key details, and parameters utilized in each part of this project.

2.1 Part 1

For Part 1, as outlined in Chapter 1, we will execute four distinct groups (Problems 1 to 4) in MOOSE:

1. Steady State w/ constant thermal conductivity k .
2. Steady State w/ temperature-dependent k .
3. Transient State w/ constant k .
4. Transient State w/ temperature-dependent k .

It's worth noting that the validity of the first group can be confirmed through comparison with the analytical solution taught in class.

2.1.1 The parameters, meshing methods, and other details

- (i) The choices of materials and their parameters:

(A) Fuel \rightarrow UO_2 : In steady state (the governing equation is

$$0 = \nabla \cdot (k \nabla T) + Q$$

When we consider the constant k , the thermal conductivity is $0.03 \text{ W cm}^{-1} \text{ K}^{-1}$ (From the lecture note); for the temperature-dependent k , the thermal conductivity (assuming the burnup FIMA=0) is

$$k_{\text{ox}} = \frac{1}{A + B * T} = \frac{1}{3.8 + 0.0217 * T}$$

In transient state, we need more parameters for our governing equation is

$$\rho c_p \left(\frac{\partial T}{\partial t} \right) = \nabla \cdot (k \nabla T) + Q$$

Therefore, we take constant $c_p = 0.33 \text{ J g}^{-1} \text{ K}^{-1}$, density = 10.97 g cm^{-3}

(B) Gap \rightarrow Pure He:

In steady state (the governing equation is

$$0 = \nabla \cdot (k \nabla T) + Q$$

When we consider the constant k , the thermal conductivity is $0.0025 \text{ W cm}^{-1} \text{ K}^{-1}$ (From the lecture note); for the temperature-dependent k , the thermal conductivity is

$$k_{\text{He}} = 1.6 \times 10^{-5} \times t^{0.79}$$

But I also set if $t < 600 \text{ s}$, $k_{\text{He}} = 0.002556 \text{ W cm}^{-1} \text{ K}^{-1}$ to avoid the error at $t = 0 \text{ s}$.

In transient state, take constant $c_p = 5.193 \text{ J g}^{-1} \text{ K}^{-1}$, density = $1.785 \times 10^{-4} \text{ g cm}^{-3}$

(C) Cladding \rightarrow Zr:

Assume the thermal conductivity of cladding is constant for our four problems,

and the value is $k_{He}=0.17 \text{ W cm}^{-1} \text{ K}$ (From the lecture note.) $c_p=0.27 \text{ J g}^{-1} \text{ K}^{-1}$,
density= 6.49 g cm^{-3}

(ii) Meshing:

Initially, I employed the GeneratedMeshGenerator to create the entire domain, while the SubdomainBoundingBoxGenerator was utilized to distinguish the fuel, gap, and cladding blocks. However, this mesh configuration posed potential issues for subsequent parts of the project. Consequently, I redefined the cladding first and separated the gap from the cladding, followed by separating the fuel from the gap. Initially, I set the number of meshes to 1000 and 100 in the x and y directions, respectively, for the entire domain. However, after considering the importance of mesh convergence testing, I determined that using 800 meshes in the x direction and 100 in the y direction provided the best fit for the analytical solution.

(iii) Others:

- a The boundary condition on the right side is defined as a Dirichlet BC with a prescribed value for the temperature outside of the cladding, $T_{co}=550 \text{ K}$. On the left side, the boundary condition is set as a Neumann BC, where the derivative of temperature normal to the boundary is zero.
- b In many examples, PJFNK solvers were commonly used, but I often encountered divergent results when employing them. Eventually, I discovered that utilizing the NEWTON solver led to efficient and convergent outcomes.

2.2 Part 2

For Part 2, we will examine the impact of the flowing coolant on the heat removal from the fuel and its resultant temperature distribution. I initially maintained the same mesh design logic as in Part 1. Then, I adjusted some dimensions of the fuel pin to meet the given conditions outlined in Part 2.

2.2.1 The parameters, meshing methods, and other details

(i) The parameters:

The parameters such as thermal conductivity are from Part 1 steady state constant k set. The mass flow rate of the coolant $\dot{m} = 0.25 \text{ kg s}^{-1}$ rod, and the coolant specific heat $C_{PW} = 4200 \text{ J kg}^{-1} \text{ K}^{-1}$ (From the lecture note)

(ii) Meshing:

We basically utilize the mesh generated in part 1 but subsequently employ the Block-DeletionGenerator to remove mesh elements within the gap block after establishing the side sets of cladding-gap and gap-fuel.

(iii) Others:

- (a) The boundary conditions on the side sets of cladding-gap and gap-fuel can be governed by the GapHeatTransfer function within the ThermalContact block.
- (b) The Dirichlet BC we employed in Part 1 now becomes a function that varies with the length of the fuel rod. Meanwhile, the Neumann BC remains unchanged.

Chapter 3

Results

3.1 Part 1

3.1.1 Analytical solution of steady state with constant k

Below is the calculation of the analytical solution:

Sol: As given, a steady state with constant k, $LHR = 350 \text{ W cm}^{-2}$, $T_{co} = 550 \text{ K}$, $R_f = R_{fuel} = 0.5 \text{ cm}$, $t_g = t_{gap} = 0.005 \text{ cm}$, $t_c = t_{cladding} = 0.1 \text{ cm}$

Take constant k, for fuel: $k_{fuel} = k_f = 0.03 \text{ W cm}^{-1} \text{ K}$, and for cladding: $k_{cladding} = k_c = 0.17 \text{ W cm}^{-1} \text{ K}$

$$\Delta T_c = T_{ci} - T_{co} = \frac{LHR}{2\pi R_f} \times \frac{t_c}{k_c} = \frac{350}{2\pi \times 0.5} \times \frac{0.1}{0.17} \approx 65.534 \text{ K}$$
$$\Rightarrow T_{ci} = 550 + 65.534 = 615.534 \text{ K}$$

The k for gap at $T = T_{ci} = 615.534 \text{ K}$ is

$$k_{gap} = k_g = 16 \times 10^{-6} \times T^{0.79} \text{ W cm}^{-1} \text{ K} = 2.556 \times 10^{-3} \text{ W cm}^{-1} \text{ K}$$

$$\Delta T_g = T_s - T_{ci} = \frac{LHR}{2\pi R_f} \times \frac{t_g}{k_g} = \frac{350}{2\pi \times 0.5} \times \frac{0.005}{0.002556} \approx 217.935 \text{ K}$$

$$\Rightarrow T_s = 615.534 + 217.935 = 833.469 \text{ K}$$

$$\Delta T_0 = T_0 - T_s = \frac{LHR}{4\pi k_f} = \frac{350}{4\pi \times 0.03} \approx 928.404 \text{ K}$$

$$\Rightarrow T_0 = 833.469 + 928.404 = 1761.873 \text{ K}$$

3.1.2 MOOSE Results

The MOOSE simulation provided temperature profile results for problems (1) to (4), along with centerline temperature versus time data for problems (3) and (4). Table 3.1 presents the temperatures of the internal cladding, the surface of the fuel pellet, and the center of the fuel for each of these problems (1) to (4).

Table 3.1: The temperature data for the internal cladding, the surface of the fuel pellet, and the center of the fuel

Temperature (K)	Steady State Constant k		Steady State Temperature-dependent k	Transient State	
	Analytical	Numerical		Constant k	Temperature-dependent k
Centerline	1761.873	1766.5	1634.23	1071.37	922.139
Surface of the fuel pellet	833.469	839.091	833.904	673.899	671.985
Inner surface of cladding	615.534	609.509	609.509	575.312	575.311

The results displayed in Figure 3.1 to Figure 3.4 of the MOOSE simulation for the four groups were adjusted following modifications to their mesh definitions and subsequent attempts at mesh convergence testing.

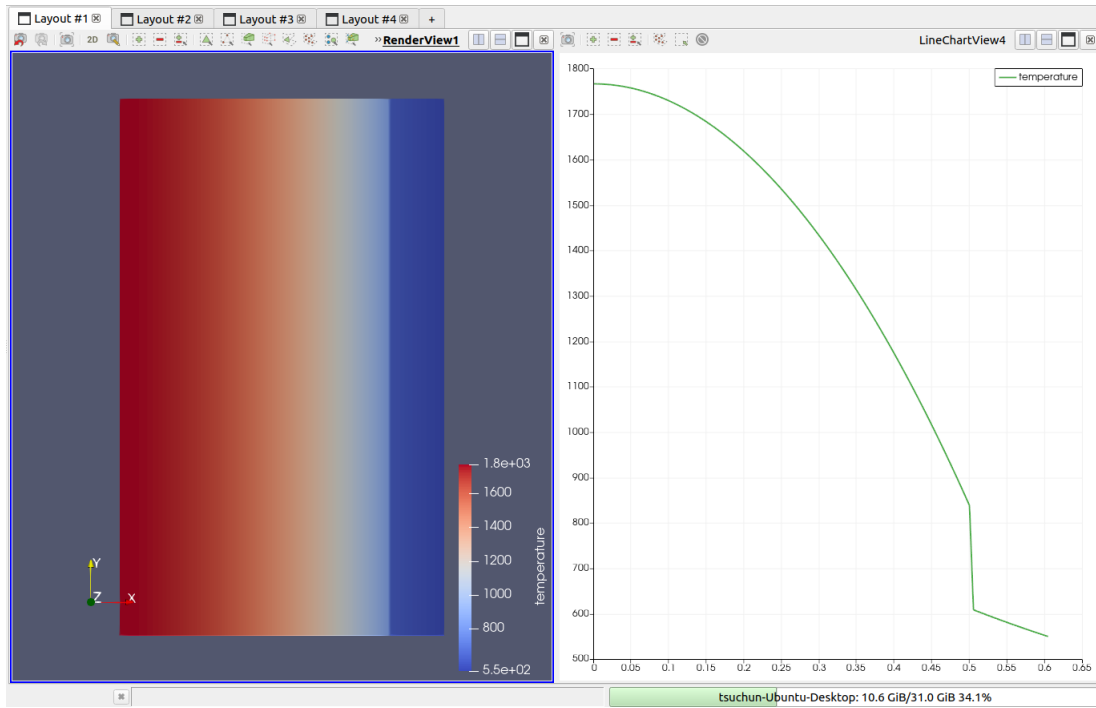


Figure 3.1: The temperature profile for Steady State Constant k (Problem (1))

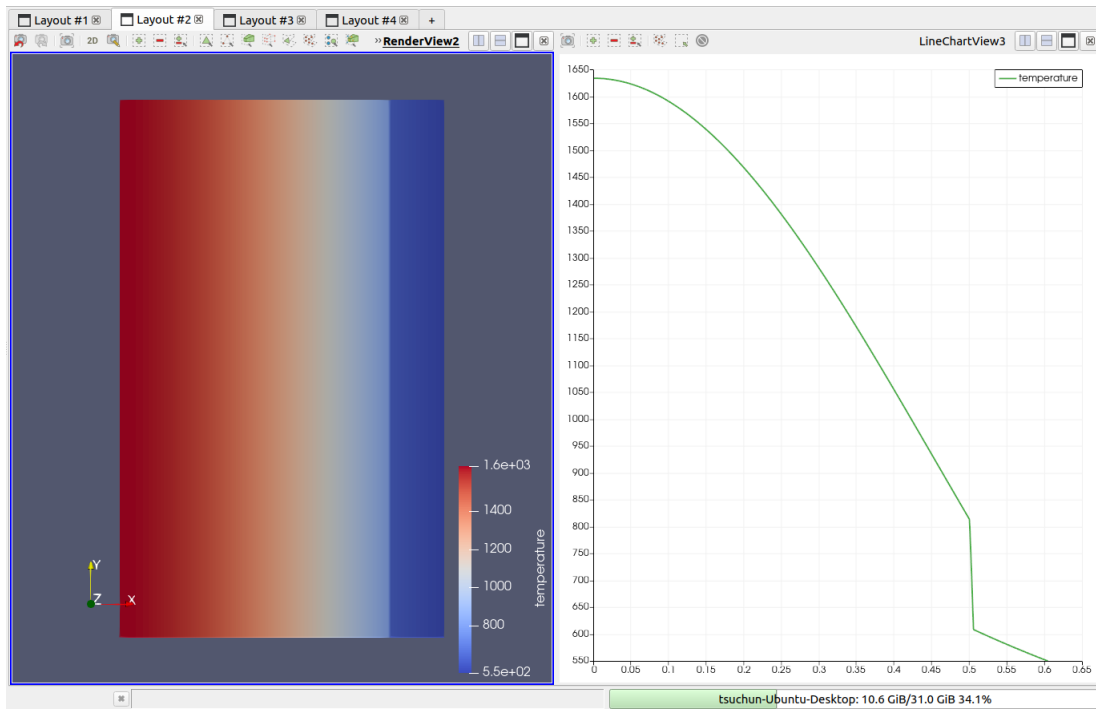


Figure 3.2: The temperature profile for Steady State Temperature-dependent k (Problem (2))

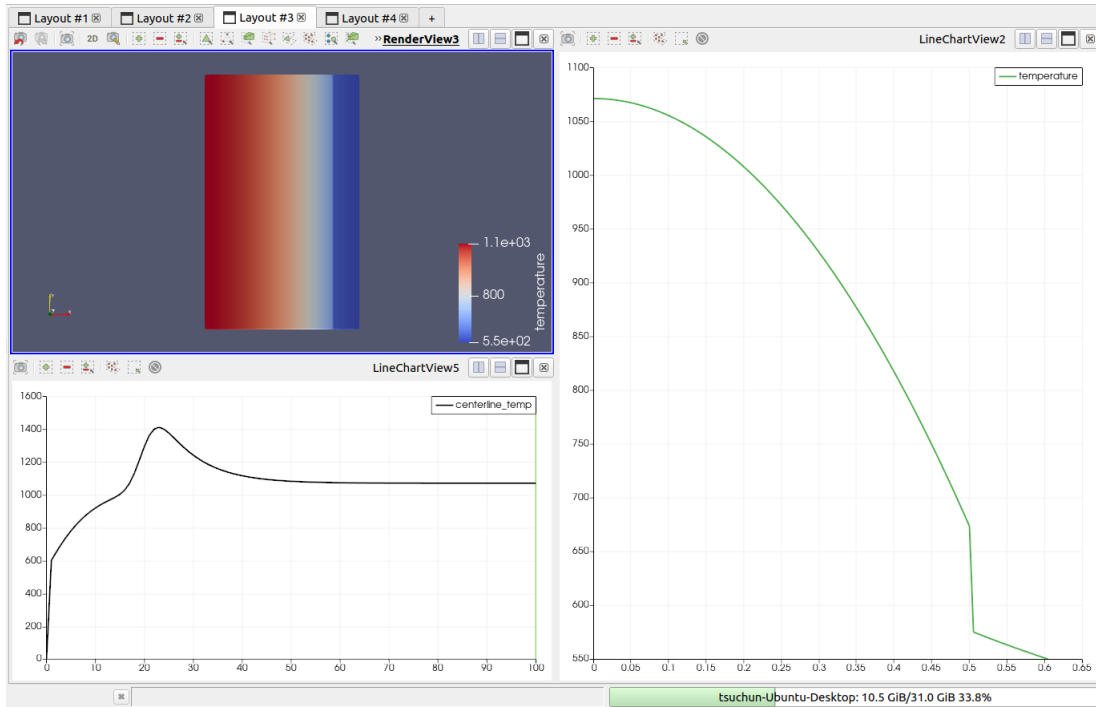


Figure 3.3: The temperature profile (Right) and the centerline temperature versus time (Lower Left) for Transient State Constant k (Problem (3))

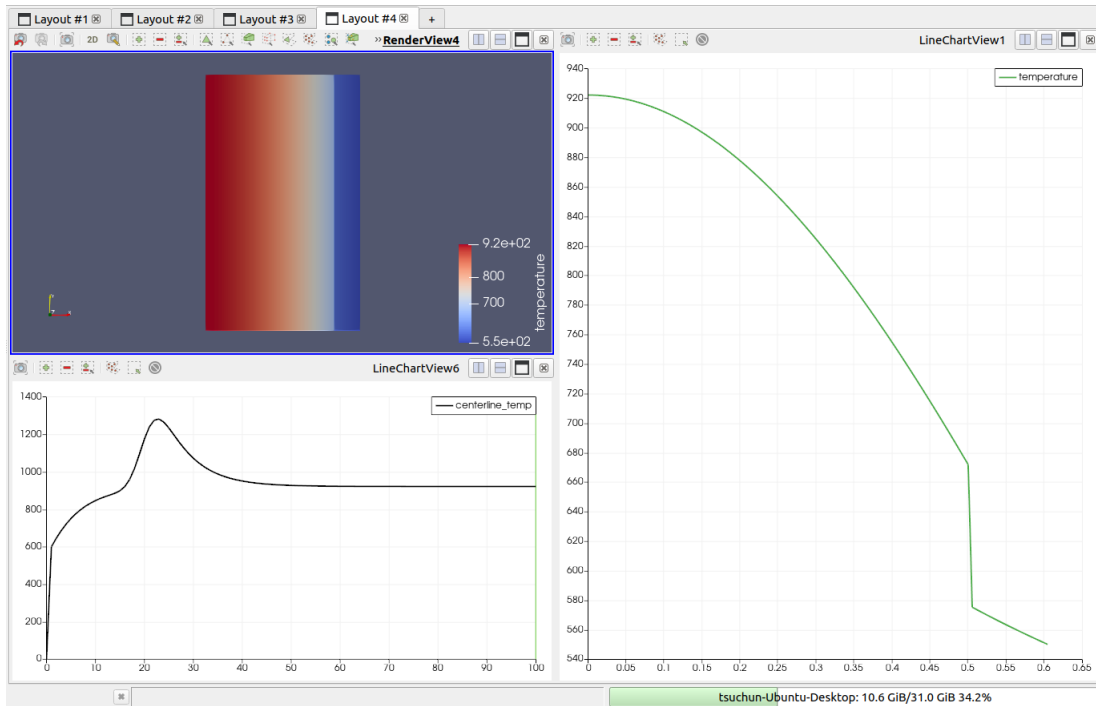


Figure 3.4: The temperature profile (Right) and the centerline temperature versus time (Lower Left) for Transient State Temperature-dependent k (Problem (4))

3.1.3 Discussion

From the Results above, we can have a brief discussion for the outcome of

- (a) When comparing the analytical solution with the MOOSE results from group 1, it's evident that selecting the number of the division of $nx = 800$ and $ny = 100$ for the finite element mesh can yield a MOOSE solution with less than 1% error.
- (b) In comparing these four groups, the crucial observation lies in whether thermal conductivity (k) is considered temperature-dependent or not. Notably, when we account for temperature dependency, significant changes in the center-line temperature are evident for both steady and transient states. However, the alterations in temperature on the surface of the fuel pellet and the inner surface of the cladding are relatively minimal.
- (c) Overall, it's notable as well that the temperature profiles from the transient states are generally lower compared to those from the steady states.

3.2 Part 2

3.2.1 MOOSE Results

For the result of the temperature profile at three different height of the rod for the steady state with constant k by MOOSE are shown in Table 3.2, and from Figure 3.5 to 3.7. The center-line temperature distribution with the axis direction is presented in Figure 3.8

Table 3.2: The temperature profile at $z = 25, 50, 100$ cm

Temperature (K)	$z = 25$ cm	$z = 50$ cm	$z = 100$ cm
Centerline	1513.96	1735.31	973.348
Surface of the fuel pellet	750.387	810.138	634.448
Inner surface of cladding	553.494	571.577	547.322
Outer surface of cladding ($T_{co} = T_{cool}$)	505.373	513.272	526.01

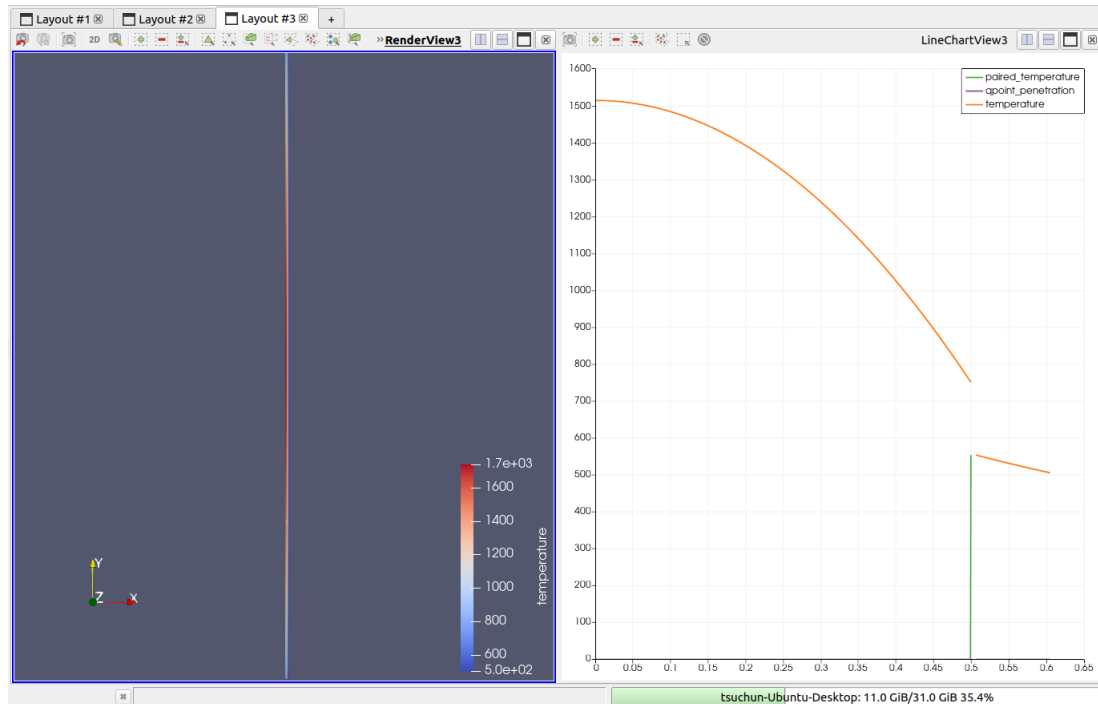


Figure 3.5: The temperature profile for Steady State Constant k at the height $z = 25$ cm

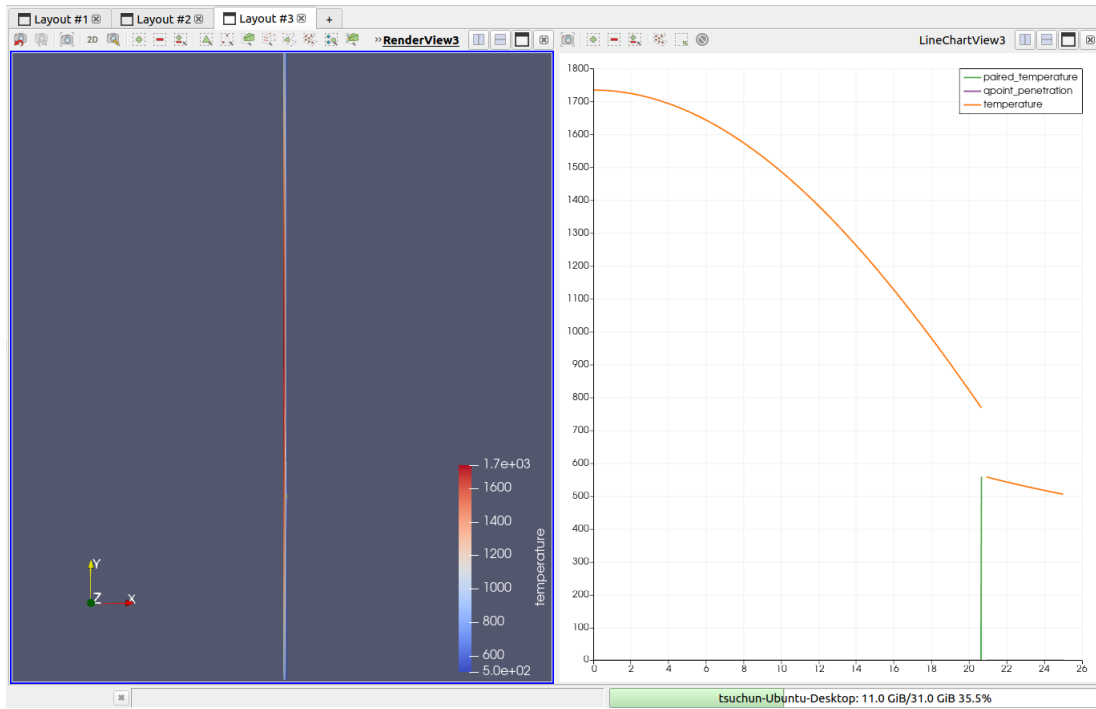


Figure 3.6: The temperature profile for Steady State Constant k at the height $z = 50$ cm

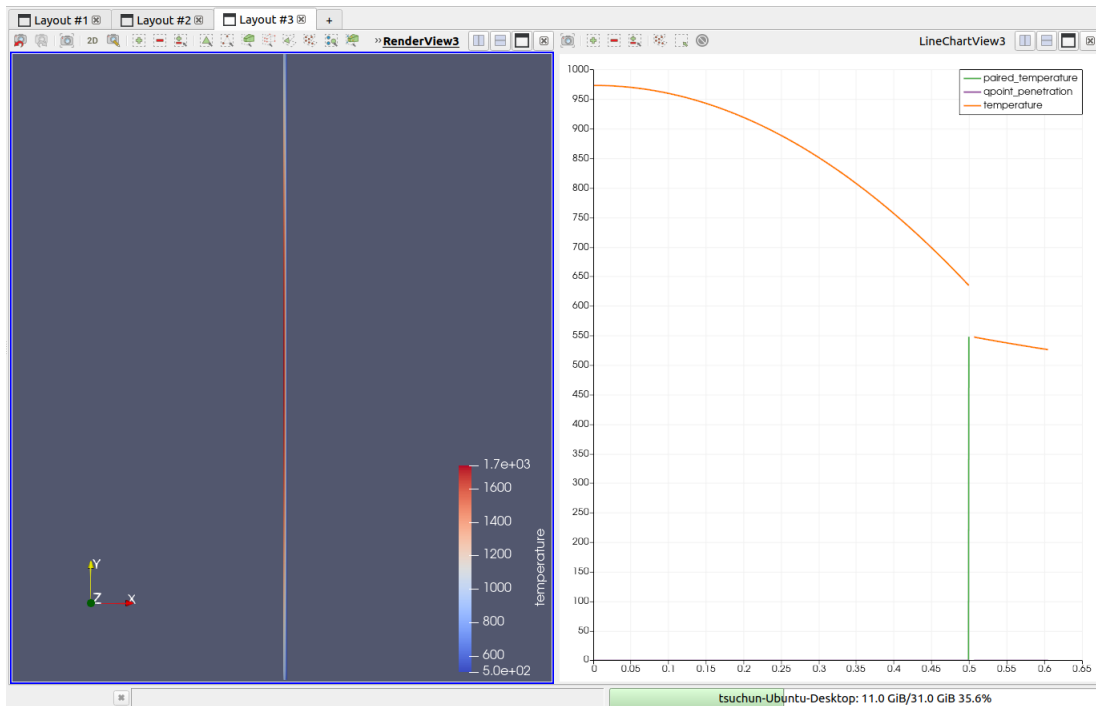


Figure 3.7: The temperature profile for Steady State Constant k at the height $z = 100$ cm

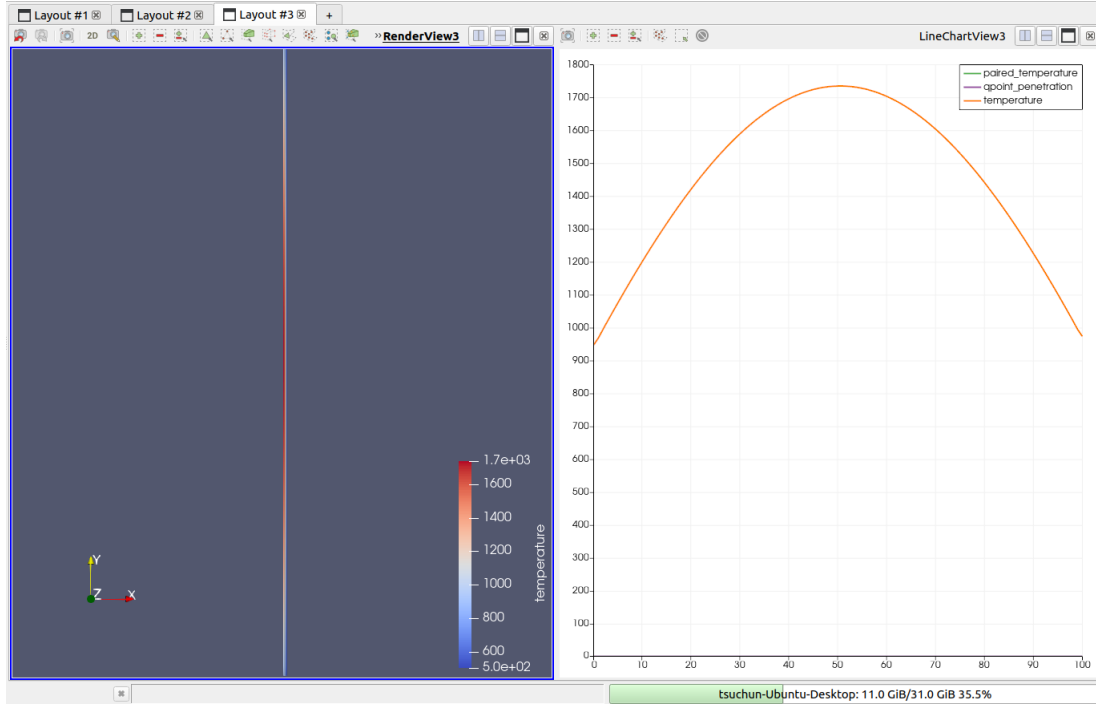


Figure 3.8: The center-line temperature in axial direction

3.2.2 Discussion

- (a) In Figure 3.5 to 3.7, the discontinuities in the temperature curves are noticeable. This occurs because we didn't directly solve for the temperature in the gap region using finite element mesh; instead, we utilized the ThermalContact method to address it.
- (b) In Lecture 3, Dr. Beeler noted that in real-world scenarios, we should expect to observe a shift of the peak of the center-line temperature to around 60% to 65% of the rod's height. However, in Figure 3.8, we only observe a slight shift, approximately at 52% of the height. One potential explanation for this inconsistency could be linked to the fact that the actual length of the fuel pin typically extends to about 3 m, and in real-world scenarios, the mass flow rate tends to be slower. Consequently, as the coolant traverses upwards towards the upper part of the fuel, it may have a higher temperature, leading to a decrease in the efficiency of heat removal.

Chapter 4

Conclusion

This project has provided us with valuable insights into practical applications and has equipped us with the ability to utilize MOOSE for solving real-world problems. From this work, we can draw several key points.

- (a) When comparing the analytical solution with the steady state results from MOOSE using constant thermal conductivity (k), it's possible to identify a mesh configuration that not only better approximates the analytical solution but also enhances the efficiency of the MOOSE simulation.
- (b) Upon considering the temperature dependency of thermal conductivity, notable changes in the center-line temperature are observed for both steady and transient states. However, the variations in temperature on the surface of the fuel pellet and the inner surface of the cladding are relatively minor. Overall, it's worth noting that the temperature profiles from the transient states tend to be lower compared to those from the steady states.
- (c) The discontinuities in the temperature curves are noticeable.(From Figure 3.5 to 3.7)
This phenomenon arises from our decision not to directly solve for the temperature in the gap region using a finite element mesh. Instead, we opted to employ the Thermal-Contact method to handle this aspect.

(d) In real-world scenarios, we should anticipate a peak of the center-line temperature shifting much higher than the result we can observe in Figure 3.8. One potential explanation for this inconsistency could be attributed to the fact that the actual length of the fuel pin typically extends to about 3 m, and in real-world scenarios, the mass flow rate tends to be slower. Consequently, as the coolant traverses upwards towards the upper part of the fuel, it may have a higher temperature, resulting in a decrease in the efficiency of heat removal.

(e) Personal Reflection on this Project:

This project presented a challenging learning curve for beginners in MOOSE. However, I view it as an incredibly positive experience. It not only introduced us to a new tool but also encouraged us to enhance our ability to filter and search for resources that aid in our understanding. This skill development is invaluable for our career growth and future research endeavors.